Photoluminescent rare earth inorganic–organic hybrid systems with different metallic alkoxide components through 2-pyrazinecarboxylate linkage

Lei Guo, Bing Yan*

Department of Chemistry, Tongji University, Siping Road 1239 Shanghai 200092, China

ARTICLE INFO

ABSTRACT

Luminescent inorganic–organic hybrid materials have been prepared by rare earth (Eu^{3+} and Tb^{3+}) 2-pyrazinecarboxylic acid complexes grafted to the different inorganic components via the chemical modification of different metallic alkoxides ($Ti(OCH(CH_3)_2)_4$ and $Al(OCH(CH_3)_2)_3$), which are characterized with FT-IR, SEM, DSC-TG and luminescence spectra, as well as luminescence decay analysis. Especially the photoluminescence measurements indicate that the 2-pyrazinecarboxylic group can sensitize rare earth (Eu^{3+} and Tb^{3+}) ions to exhibit characteristic luminescence in different hybrid hosts. The photoluminescence behaviours of Eu^{3+} hybrid materials ($^5D_0$–$^7F_0$ energy, the ratios of red/orange, $^5D_0$ quantum efficiency and number of coordinated water molecules) are investigated in detail and a maximum quantum efficiency of 12.9% is found for hybrid material Eu-PZC-Al.

1. Introduction

The concept of inorganic–organic hybrid systems emerged in the last three decades, with the advent of "soft" inorganic chemistry processes, in particular the sol–gel route [1,2]. This kind of systems have attracting a great deal of attention because they can combine the mutual advantages of both inorganic matrix and organic molecule. The very large range of choices for the inorganic and organic components offers the possibility of obtaining systems with attractive performances such as mechanical, thermal, and other physical and chemical properties [3,4]. It is well-known that some rare earth complexes (especially Eu^{3+}, Tb^{3+}, Sm^{3+} and Dy^{3+}) show sharp characteristic photoluminescence bands upon ultraviolet light irradiation because of the energy transfer from the ligands to the central rare earth ions. So, entrapping rare earth complexes with different organic ligands (such as β-diketones, aromatic carboxylic acids, and heterocyclic ligands) in sol–gel-derived host systems has been studied to improve the thermal stability and mechanical property of the rare earth complexes [5–7]. According to the interaction among the different components in hybrid systems, these hybrid systems can be mainly classified into two major classes: one is physically mixed with weak interactions (hydrogen bonding, van der Waals force, or weak static effect) between the inorganic and organic component and the other is chemically bonding of the complex to the inorganic matrix [8–10]. The latter hybrid materials belong to the molecular-based systems, which can exhibit monophasic appearance even at a high concentration of rare earth complexes. The design of new luminescent hybrid systems based on chemically bonded rare earth complexes is a very active research field at the present [11–15]. Our research group is dedicated to the design of the rare earth luminescent hybrid systems covalently boned with inorganic networks [16–19].

However, luminescent inorganic–organic hybrid systems grafted with rare earth complexes are focused mainly on siloxane-based hybrid networks. The research about the other inorganic matrices hybrid systems such as titania, zirconia, and aluminum hybrid networks is rarely reported. Thus, it would be highly attractive to investigate luminescence properties of the rare earth complex grafted to the different metallic alkoxides matrix. Besides, europium complexes can be immobilized on titania via chemical modification of titanium alkoxide [20,21]. This not only will result in systems with interesting properties but also is a case study on the chemical possibilities to tether metal complexes to nonsilicate metal oxides. The extension of this kind of hybrid systems to metal oxides other than silica would allow interesting new options for the development of inorganic–organic hybrid systems [22–25].

As we known, the organic and inorganic groups that linked by stable chemical bonds require precursors in which the organic group (R) is bonded to the oxide-forming element in a hydrolytically stable way. Typical examples are organically substituted alkoxysilanes R–Si(OR′)$_3$, in which the group R is bonded to silicon via a Si–C bond [26–29]. Design this organically substituted

---

* Corresponding author. Tel.: +86 21 65984663; fax: +86 21 65982287.
E-mail address: byan@tongji.edu.cn (B. Yan).

alkoxysilanes also can be recognized the key procedure to construct molecular-based hybrid systems, which can behave double functions of both coordinating to rare earth ions and sol–gel processing to constitute a covalent Si–O network. However, rare earth complexes cannot be linked to the titanium and aluminum centers as with silicon due to the hydrolytic cleavage of Ti–C and Al–C bonds [20]. Therefore, a new method has to be developed for grafting rare earth complexes to different inorganic matrix. In this work, 2-pyrazinecarboxylic acid ligand is selected to construct the linkage between inorganic matrix and rare earth ions. The carboxylic acid group of it can react with metallic alkoxide to moderate the reactivity toward hydrolysis and condensation, while the heterocyclic group can coordinate to rare earth ions as well as sensitize the luminescence of them. In this way, rare earth complexes can be anchored within the framework of inorganic–organic hybrid systems. The resulting hybrid systems are characterized and the photophysical properties of them are also investigated and compared in detail.

2. Experimental

2.1. Materials

The purity of rare earth oxide exceeds 99.99%. Rare earth nitrates hexahydrate are prepared by dissolving the corresponding oxides in dilute nitric acid, then heating the solution appropriately. All of the other reagents are analytically pure and solvents are purified according to literature procedures [30].

2.2. Physical measurements

Rare earth contents of the complexes were determined by EDTA titration using Xylenol-orange as an indicator. Elemental analyses (C, H, N) were determined with an Elementar Cario EL elemental analyzer. Fourier transform infrared spectra are recorded on KBr disk using Nicolet model 5SXC spectrometer in $4000–400\,cm^{-1}$ region. The X-ray diffraction (XRD) measurements are carried out on powdered samples via a BRUKER D8 diffractometer ($40\,mA/40\,kV$), using monochromated Cu Kα_1 radiation ($\lambda = 1.54\,\text{Å}$) over the 2θ range of $10–70°$. Differential scanning calorimetry (DSC) and thermogravimetric analysis (TG) are performed on a NETZSCH STA 449C at a heating rate of $15\,°C/min$ under a nitrogen atmosphere. Scanning electronic microscope (SEM) images are obtained with a Philips XL-30. The ultraviolet–visible diffuse reflection spectra of the powder samples are recorded by a BWS003 spectrophotometer. Luminescence excitation and emission spectra are obtained on a SHIMADZU RF-5301 spectrofluorimeter. Luminescent lifetimes are determined on an Edinburgh Instruments FLS 920 phosphorimeter, using a 150 W xenon lamp as the excitation source (pulse width, 3 μs). All measurements are performed at room temperature except the luminescent lifetimes.

Synthesis of hybrid materials RE-PZC-Ti, RE-PZC-Al and RE-PZC-Ti-Al (RE = Eu and Tb): A sample is prepared by adding 4 mmol of $Ti(OCH(CH_3)_2)_4$ ($Al(OCH(CH_3)_2)_3$) to 20 mL of EtOH containing 4 mmol of 2-pyrazinecarboxylic acid ligand under refluxing and stirring. 1 mmol of $RE(NO_3)_3 \cdot 6H_2O$ (RE = Eu^{3+} and Tb^{3+}) dissolved in EtOH is added dropwise into the clear solution and 0.1 mL H_2O is then added. The stirring is continued for another 1 h to yield a white precipitate, which is recovered by centrifugation and dried for 24 h at 65 °C under vacuum. The sample is named RE-PZC-Ti and RE-PZC-Al. The predicted structure of obtained hybrid materials is shown in Fig. 1. A sample RE-PZC-Ti-Al is prepared using the similar method except that the 4 mmol of $Ti(OCH(CH_3)_2)_4$ or $Al(OCH(CH_3)_2)_3$ is replaced by 2 mmol of $Ti(OCH(CH_3)_2)_4$ and
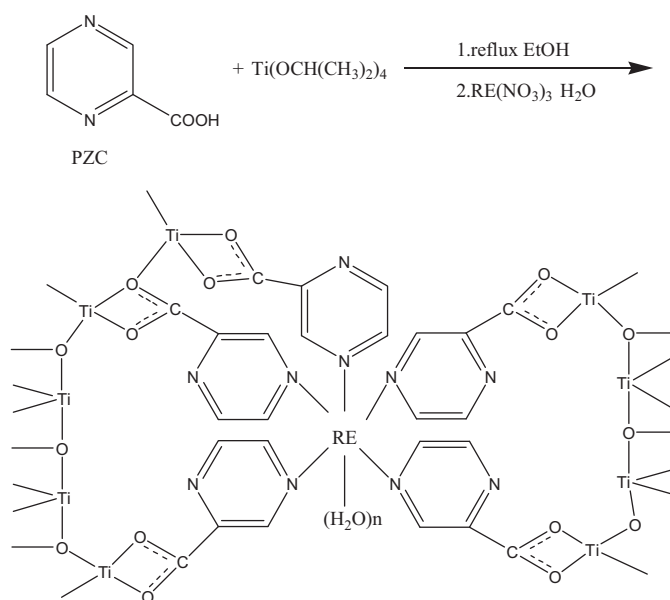

Fig. 1. The scheme for the synthesis processes and predicted structure of hybrid system RE-PZC-Ti.

2 mmol of $Al(OCH(CH_3)_2)_3$. Anal. Calcd. For Eu-PZC-Ti (%): C 20.79, H 1.73, N 12.61, Eu 10.53; Found: C 20.58, H 2.23, N 13.04, Eu 10.95; for Tb-PZC-Ti (%): C 20.69, H 1.72, N 12.55, Eu, 10.97; Found: C 20.35, H 2.18, N 12.91, Eu 11.25, corresponding to the formula $(TiO_2)_5(C_5H_4N_2O_2)_5RE(NO_3)_3(H_2O)_{4.5}$, RE = Eu, Tb. For Eu-PZC-Al (%): C 23.43, H 1.80, N 14.21, Eu 11.87; Found: C 23.07, H 1.98, N 15.05, Eu 12.33; for Tb-PZC-Al (%): C 23.30, H 1.79, N 14.14, Eu, 12.35; Found: C 23.11, H 2.01, N 14.86, Eu 12.60, corresponding to the formula $(Al_2O_3)_{2.5}(C_5H_4N_2O_2)_5RE(NO_3)_3(H_2O)_5$, RE = Eu, Tb. For Eu-PZC-Ti-Al (%): C 22.18, H 1.70, N 13.45, Eu 11.24; Found: C 21.82, H 2.12, N 13.87, Eu 12.06; for Tb-PZC-Ti-Al (%): C 22.06, H 1.69, N 13.38, Eu, 11.69; Found: C 21.85, H 2.04, N 13.81, Eu 12.11, corresponding to the formula $(Al_2O_3)_{1.25}(TiO_2)_{2.5}(C_5H_4N_2O_2)_5RE(NO_3)_3(H_2O)_5$, RE = Eu, Tb. The calculated values of them are based on the formula with the complete hydrolysis and condensation to form the inorganic network. However, the sol–gel reaction cannot be guaranteed to be completely and so it is difficult to determine the exact composition of the obtained hybrid materials within the complicated hybrid system. So there exists a large distinction between the found data and calculated value.

3. Results and discussion

According to the previous work [20,31,32], the carboxylic acid group can react with metallic alkoxides to moderate the reactivity toward hydrolysis and condensation. Herein, the ligand 2-pyrazinecarboxylic acid not only can coordinate to rare earth ions and sensitize the luminescence of them, but also can anchor the rare earth complexes to the framework of inorganic–organic titania or alumina matrix. The FTIR spectra of Eu-PZC-Ti, Eu-PZC-Al and Eu-PZC-Ti-Al are shown in Fig. 2 (I). The complexation reaction are demonstrated by the red shift of C=O stretching vibration from $1725\,cm^{-1}$ [33] to about $1650\,cm^{-1}$. A broad band located at about $3370\,cm^{-1}$ attributed to $\nu_{(O-H)}$ of H_2O molecule in the hybrid materials. This is in good agreement with the results reported previously [20,21]. In addition, a strong and broad band in the range of $500–900\,cm^{-1}$, due to Ti–O–Ti and Al–O–Al stretching vibration modes [34,35]. The FTIR spectra of Tb-containing materials are similar to those of the above Eu-containing hybrid materials
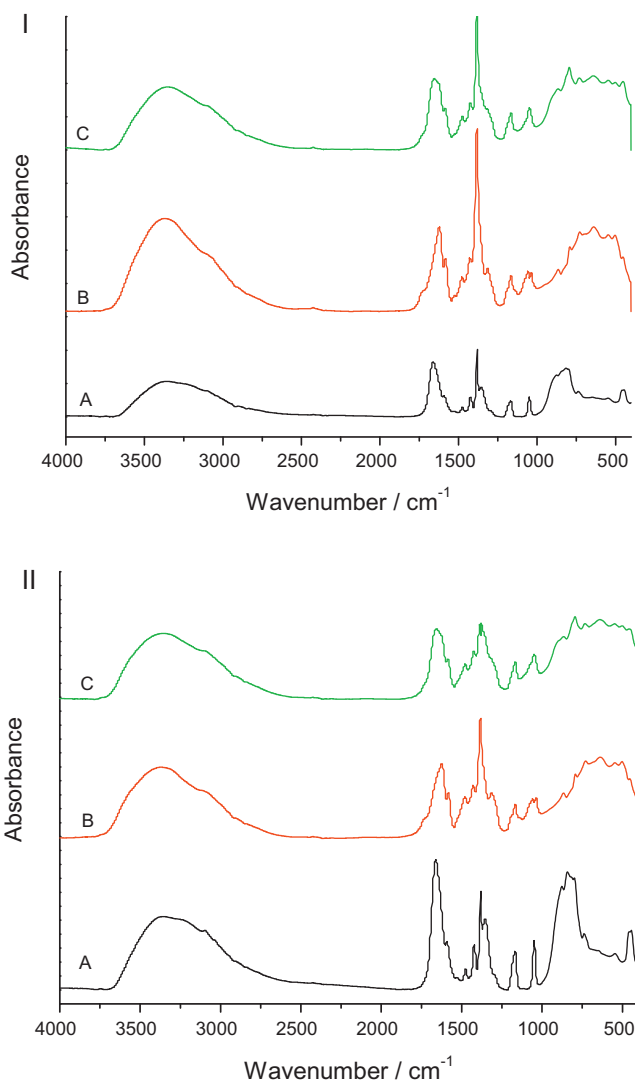
Fig. 3. Differential scanning calorimetry (DSC) and thermogravimetric (TG) curves of hybrid systems Eu-PZC-Ti and Eu-PZC-Al.

and 2.47% (Eu-PZC-Al: about 1.8 molecular H_2O) for this thermal event is revealed by the TG curve, and it is in good agreement with the results reported it is calculated that there are approximately 2.6 molecular H_2O in one. Then, the weight loss between about 320 °C and 460 °C is assigned to the decomposition of organic ingredients. The total mass loss up to 1000 °C is 40%. These results are similar to those achieved with systems containing silica as inorganic matrix [36,37], so the choice of the inorganic matrix other than silica becomes more extensive and more multifunctional luminescent hybrid systems could be obtained.

The UV–vis diffuse reflection absorption spectrum of the PZC-Ti and excitation spectra of the hybrid materials RE-PZC-Ti (RE = Eu and Tb, monitored at 614 and 545 nm, respectively) are shown in Fig. 4. The overlaps can be observed between the absorption band of PZC-Ti (a) and the excitation bands of RE-PZC-Ti (b for Eu-PZC-Ti and c for Tb-PZC-Ti), which indicates that in the hybrid materials the central RE^{3+} ion can be efficiently sensitized by the ligand through the so-called antenna effect [38–40]. The other overlaps between the absorption spectrum of the ligand (PZC-Al and PZC-Ti-Al) and the excitation spectra of the corresponding hybrid materials, which are provided in Supporting Information (Figs. S2

Fig. 2. Infrared spectra of (I) Eu^{3+}-containing hybrid systems: (A) Eu-PZC-Ti, (B) Eu-PZC-Al and (C) Eu-PZC-Ti-Al; and (II) Tb^{3+}-containing hybrid systems: (A) Tb-PZC-Ti, (B) Tb-PZC-Al and (C) Tb-PZC-Ti-Al.

(Fig. 2 (II)). All the systems obtained are amorphous as revealed by XRD patterns (not shown). The scanning electron micrographs (SEM) of the obtained Eu^{3+}-containing hybrid materials are given in Fig. S1. Comparing the three SEM pictures, there exist differences between the three kinds of hybrid materials despite the fact that they are prepared by the same process, which may be assigned to the difference of the metallic alkoxides matrix. The morphology of system Eu-PZC-Ti is aggregates of small particles with dimensions up to 0.5–1 μm, while much larger particles tending to form aggregates can be observed in Eu-PZC-Al and Eu-PZC-Ti-Al systems. In addition, the terbium-containing hybrid materials show the similar microstructure (not shown), suggesting the rare earth ions hardly affect the microstructure in these hybrid materials.

The thermal stability of all obtained hybrid materials is demonstrated by DSC-TG measurement. Fig. 3 shows the DSC and TG curves of Eu-PZC-Ti and Eu-PZC-Al materials. From Fig. 3 we can see that both of the samples show the similar change trends in weight loss and thermal process. Their slight differences of weight loss may be due to the different inorganic matrix and the different degrees of polycondensation reaction. In curves of TG, water molecular is removed by an endothermic effect at low temperature, centered at 76 °C. The mass loss of 3.75% (Eu-PZC-Ti: about 3.0 molecular H_2O)
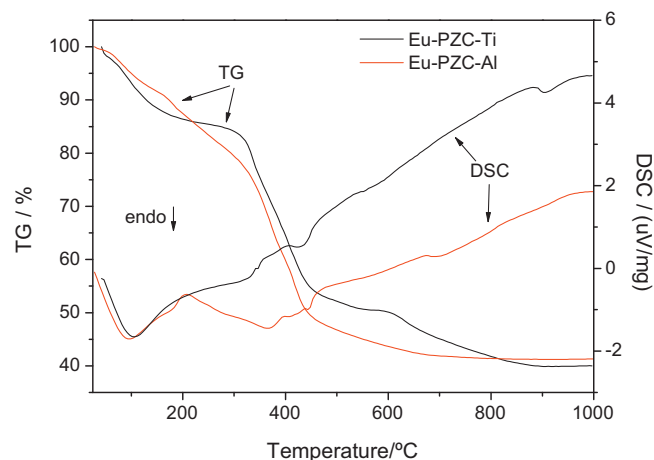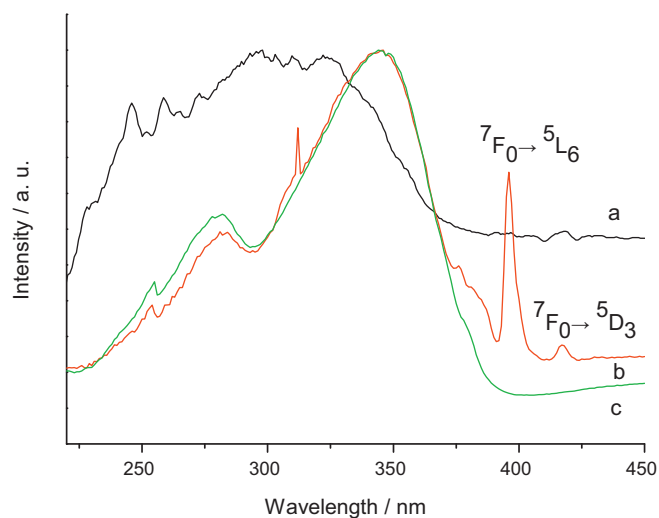

Fig. 4. DR UV–vis absorption spectrum of PZC-Ti (a) in the solid; excitation spectra for Eu-PZC-Ti (b) and Tb-PZC-Ti (c) monitored at 614 and 545 nm in the solid, respectively. All spectra are normalized to a constant intensity at the maximum.
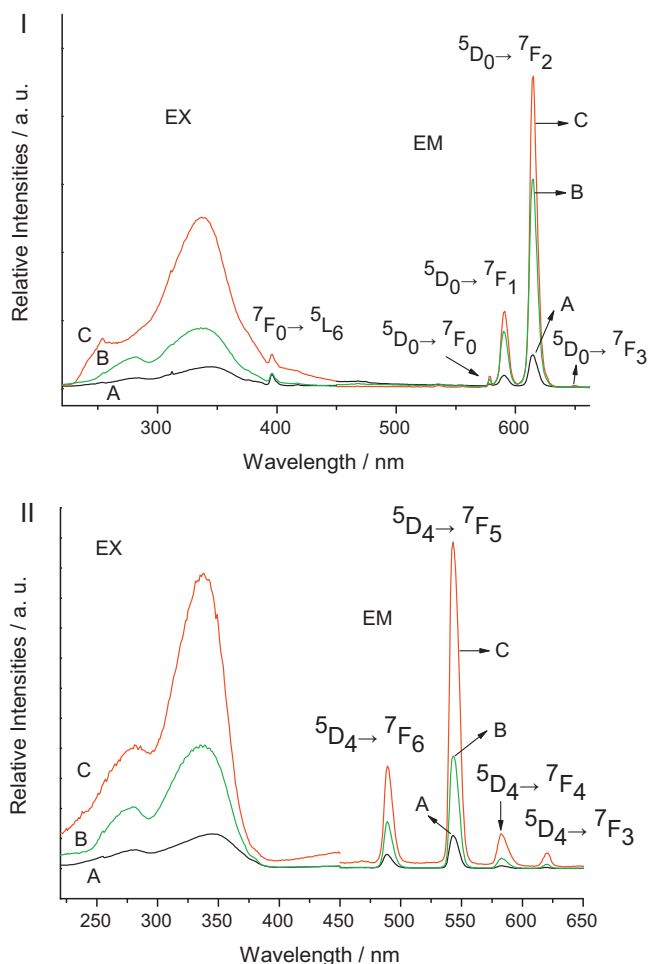
Fig. 5. Excitation and emission spectra for europium (I) and terbium (II) hybrid systems (A: RE-PZC-Ti; B: RE-PZC-Ti-Al; C: RE-PZC-Al).

Table 1
Lifetime (τ, μs), value of I_{02}/I_{01}, quantum efficiency (η), radiative (A_{rad}) and nonradiative (A_{nrad}) transition probabilities of the $^5D_0$ level and number of water molecules coordinated to the Eu^{3+} ion (n_w) for europium hybrid materials.

Hybrids	Eu-PZC-Ti	Eu-PZC-Al	Eu-PZC-Ti-Al
τ (μs)	352.7 ± 0.6	478.6 ± 0.5	421.3 ± 0.1
I_{02}/I_{01}	2.99	4.10	4.00
A_{rad} (ms^{-1})	0.212	0.269	0.266
A_{nrad} (ms^{-1})	2.621	1.719	2.109
η (%)	7.5	12.9	11.2
n_w	2.6	1.7	2.0
Ω_2 ($\times 10^{-20}$ cm^2)	4.52	6.18	6.05

the hybrid systems. The emission spectra for the Tb^{3+}-containing hybrid systems are exhibited in Fig. 5 (II). Similarly to the optical features of Eu^{3+} hybrid systems, the emission spectra obtained after excitation at 338 nm contains four intense emission lines of Tb^{3+}, peaking at 489 ($^5D_4$–$^7F_6$), 543 ($^5D_4$–$^7F_5$), 583 ($^5D_4$–$^7F_4$) and 620 nm ($^5D_4$–$^7F_3$), with the $^5D_4$–$^7F_5$ green emission as the most prominent peak.

In order to further investigate the influence of the different metallic alkoxide component in the photoluminescence features of the respective hybrid systems, the intensity (the integration of the luminescent band) ratio of the $^5D_0$–$^7F_2$ transition to the $^5D_0$–$^7F_1$ transition are analyzed in greater detail; As we known, the $^5D_0$–$^7F_1$ transition is a magnetic-dipolar transition and is insensitive to the local structure environment, whereas the $^5D_0$–$^7F_2$ transition is an electric-dipolar transition and is sensitive to the coordination environment of the Eu^{3+} ion. In these europium hybrid systems, the intensity ratios $I_{02}(^5D_0$–$^7F_2)/I_{01}(^5D_0$–$^7F_1)$ are 2.99, 4.10, and 4.00 respectively. This ratio is only possible when the europium ion does not occupy a site with inversion symmetry [43]. These data reflect the actual coordination environment of the Eu^{3+} and interpret the predicted structure (Fig. 1). Further evidence of a single local Eu^{3+} coordination environment is given by the presence of a single line for the nondegenerated $^5D_0$–$^7F_0$ transition, whose energy (E_{00}) and full-width at half maximum ($fwhm_{00}$) values are estimated by fitting a single Gaussian function. The E_{00} and $fwhm_{00}$ values are, respectively, 17289.5 ± 0.3 cm^{-1} and 66.7 ± 3.6 cm^{-1} for Eu-PZC-Ti, 17285.3 ± 0.3 cm^{-1} and 48.0 ± 0.6 cm^{-1} for Eu-PZC-Al and 17291.1 ± 0.8 cm^{-1} and 81.7 ± 1.8 cm^{-1} for Eu-PZC-Ti-Al. The similar E_{00} values indicate that the Eu^{3+} ions occupy the same average local environment in each material. However, the larger $fwhm_{00}$ value found for the hybrid material with titania as matrix points out a larger distribution of Eu^{3+} local environments in the presence of Ti [44–46].

Furthermore, the lifetime values of the $^5D_0$ (Eu^{3+}) and $^5D_4$ (Tb^{3+}) excited states are estimated on the basis of the emission decay curves monitored within the more intense Eu^{3+} ($^5D_0$–$^7F_2$) and Tb^{3+} ($^5D_4$–$^7F_5$) transitions, respectively, and under direct 336 nm and 338 nm excitation. All the curves reveal a single exponential behaviour (not shown), which corroborates that all the rare earth ions occupy the same average local environment within each hybrid materials. For the Eu^{3+}-containing hybrid materials, the obtained lifetime values are given in Table 1. For the Tb^{3+}-containing hybrid materials, the $^5D_4$ lifetime of these materials are 335.5 ± 1.1 μs (Tb-PZC-Ti), 341.2 ± 0.02 μs (Tb-PZC-Al) and 553.0 ± 3.3 μs (Tb-PZC-Ti-Al), respectively.

The $^5D_0$ quantum efficiency (η) and the detailed luminescent data for Eu^{3+} hybrid materials can be estimated on the basis of the emission spectrum and lifetime of the $^5D_0$ state by using the following equations according to Ref. [47]. The $^5D_0$ quantum efficiency of the luminescence step, η expresses how well the radiative processes (characterized by rate constant Ar), competes with nonradiative processes (overall rate constant Anr). Assuming that only

and S3), also imply that the RE^{3+} ions in the hybrid systems can be efficiently sensitized by the ligand.

Fig. 5 shows the excitation and emission spectra of the obtained hybrid materials excited under UV radiation. For the Eu^{3+}-containing hybrid materials the excitation spectra present a large broad band in the range of 310–360 nm ($\lambda_{\max}$ at about 337 nm) and of a series of intra-$4f_6$ lines, namely, between the $^7F_0$ and the $^5L_6$, $^5D_3$, levels. The broad band can be mainly ascribed to transitions involving the π–π^* states of the organic ligand [41,42]. Compared with the absorption intensity of organic ligand, the intra-4f lines are too weak, proving that luminescence sensitization via excitation of ligand is much more efficient than direct excitation of the absorption levels of the Eu^{3+} ions. For the Tb^{3+} hybrid materials a similar broad band is also detected.

In the emission spectra of the obtained hybrid materials, all the spectra are composed of a series of straight lines ascribed to the Eu^{3+} $^5D_0$–$^7F_{0-3}$ transitions and assigned to the Tb^{3+} $^5D_4$–$^7F_{6-3}$ transitions. Fig. 5 (I) illustrates the typical emission spectra of the europium hybrid systems. The four prominent emission peaks at 578, 591, 614 and 650 nm in the emission spectra can be attributed to the $^5D_0$–^7F_J ($J = 0$–3) transition with red emission for $J = 2$ as the dominant feature. There is no evidence for emission from the triplet state of the 2-pyrazinecarboxylic acid (no broad band emission observed in the blue and green spectral regions). This indicates that there is an efficient energy transfer from the triplet states of the organic ligands to the central europium ion. In addition, similar behaviour is also observed when Eu^{3+} is replaced by Tb^{3+} in

nonradiative and radiative processes are involved in the depopulation of the $^5D_0$ state, η may be defined as:

$$\eta = \frac{Ar}{(Ar + Anr)} \tag{1}$$

The radiative contribution may be calculated from the relative intensities of the $^5D_0-^7F_{0-4}$ transitions (the $^5D_0-^7F_{5,6}$ branching ratios are neglected due to their poor relative intensity with respect to that of the remaining $^5D_0-^7F_{0-4}$ lines). The $^5D_0-^7F_1$ transition does not depend on the local ligand field and thus may be used as a reference for the whole spectrum, in vacuum $A_{0-1} = 14.65\,s^{-1}$. An effective refractive index of 1.5 is used leading to $A(^5D_0-^7F_1) \approx 50\,s^{-1}$ [48,49]. The values found for η, Ar and Anr are gathered in Table 1. Comparing the η values of the obtained materials with different inorganic matrix, we can see that the η values are determined in the order: Eu-PZC-Al (12.9%) > Eu-PZC-Ti-Al (11.2%) > Eu-PZC-Ti (7.5%). Such an order is due to both a larger I_{02}/I_{01} (red/orange ratio) and the lifetime value of the hybrid Eu-PZC-Al. However, comparing the η values of the obtained hybrid materials with those previously reported for the inorganic–organic titania systems [20] the value of titania system in this work are smaller. In spite of the similar lifetime value and Anr value are obtained, Eu-PZC-Ti display much lower Ar value relative to those known for the titania systems. Comparing the Eu-PZC-Ti hybrid with the Eu-PZC-Ti-Al hybrid, an increase in the η values is observed. For the case of hybrid Eu-PZC-Ti-Al, after incorporation of the alumina matrix, an increase in the lifetime value of the $^5D_0$ and radiative transition probability Ar is observed. On the basis of these results, we may presume that the presence of the alumina inorganic matrix play the role of sensitization for the luminescence properties of obtained hybrid materials in this hybrid system.

The variations in η and Anr values may be rationalized in terms of the number of water molecules coordinated to the Eu^{3+} ions (n_w) based on the empirical formula reported by Supkowski and Horrocks [50].

$$n_w = 1.11 \times (\tau^{-1} - Ar - 0.31) \tag{2}$$

The results obtained for these hybrid materials are shown in Table 1. The estimated values are 2.6, 1.7 and 2.0 for the Eu-PZC-Ti, Eu-PZC-Al and Eu-PZC-Ti-Al materials, respectively. From these results, it is reasonable to assume that the number of water molecules coordinated to the Eu^{3+} is about 2–3. The coordination water molecules produce the severe vibration of the hydroxyl group, resulting in the large nonradiative transition and decreasing the luminescent efficiency. This is also a reason for that the titania hybrid system have the smaller η value.

As we known, the Judd–Ofelt (J–O) theory is one of the most successful theories to analyze the radiative transition within the $4f^N$ configuration of a RE^{3+} ion in host matrix based on its room temperature optical absorption measurement. To further characterize the Eu^{3+}-local coordination the experimental values for the Ω_2 intensity parameters are determined (Table 1) following a method detailed elsewhere [1]. It is known that the parameter of Ω_2 is associated with short-range coordination effects and its value increases with the basic character of the ligand, increasing coordination number, decreasing site symmetry and decreasing metal–ligand bond lengths [51]. In these results the Ω_2 values increase slightly as the incorporation of the alumina matrix, which might be interpreted as a consequence of the hypersensitive behaviour of the $^5D_0-^7F_2$ transition, suggesting that the dynamic coupling mechanism is quite operative and that the chemical environment is highly polarizable [52].

4. Conclusions

In this work we are able to synthesize new rare earth inorganic–organic hybrid systems by different metallic alkoxides ($Ti(OCH(CH_3)_2)_4$ and $Al(OCH(CH_3)_2)_3$) chemically bonded with 2-pyrazinecarboxylic acid ligand. The Eu^{3+} and Tb^{3+}-containing systems show the typical red and green emissions, respectively, while the organic ligand can efficiently sensitize RE^{3+} ions in the hybrid systems. The different inorganic matrix has some influence on the microstructure, especially on the photophysical properties such as luminescent lifetimes and $^5D_0$ quantum efficiencies. The hybrid materials with the alumina inorganic matrix have the higher $^5D_0$ quantum efficiency than that of the titania hybrid systems. Furthermore, the current design method can be conveniently applied to other hybrid systems. The desired properties can be tailored by an appropriate choice of the inorganic matrix and organic ligands.

Appendix A. Supplementary data

Supplementary data associated with this article can be found, in the online version, at doi:10.1016/j.jphotochem.2011.09.018.

References

[1] L.D. Carlos, R.A. Sá Ferreira, V.D. Bermudez, S.J.L. Ribeiro, Lanthanide-containing light-emitting organic–inorganic hybrids. A bet on the future, Adv. Mater. 21 (2009) 509–534.
[2] H. Schmidt, Considerations about the sol–gel process: from the classical sol–gel route to advanced chemical nanotechnologies, J. Sol–Gel Sci. Technol. 40 (2006) 115–130.
[3] M. Schneider, K. Muller, Hybrid materials doped with covalently bound perylene dyes through the sol–gel process, Chem. Mater. 12 (2000) 352–362.
[4] C. Molina, K. Dahmouche, C.V. Santilli, A.F. Craievich, S.J.L. Ribeiro, Structure and luminescence of Eu^{3+}-doped class I siloxane-poly(ethylene glycol) hybrids, Chem. Mater. 13 (2001) 2818–2823.
[5] D.M. Wang, J.H. Zhang, Q. Lin, L.S. Fu, H.J. Zhang, B. Yang, Lanthanide complex/polymer composite optical resin with intense narrow band emission, high transparency and good mechanical performance, J. Mater. Chem. 13 (2003) 2279–2284.
[6] Y. Wang, H.R. Li, Y. Feng, H.J. Zhang, G. Calzaferri, T.Z. Ren, Orienting zeolite L microcrystals with a functional linker, Angew. Chem. Int. Ed. 49 (2010) 1434–1438.
[7] R.F. Martins, R.F. Silva, R.R. Gonçalves, O.A. Serra, Luminescence in colorless, transparent, thermally stable thin films of Eu^{3+} and Tb^{3+} beta-diketonates in hybrid inorganic–organic zinc-based sol–gel matrix, J. Fluoresc. 20 (2010) 739–743.
[8] C. Sanchez, F. Ribot, Design of hybrid organic–inorganic materials synthesized via sol–gel chemistry, J. Chem. 18 (1994) 1007–1047.
[9] C. Sanchez, F. Ribot, B. Lebeau, Molecular design of hybrid organic–inorganic nanocomposites synthesized via sol–gel chemistry, J. Mater. Chem. 9 (1999) 35–44.
[10] P.N. Minoofar, R. Hernandez, S. Chia, B. Dunn, J.I. Zink, A.C. Franville, Placement and characterization of pairs of luminescent molecules in spatially separated regions of nanostructured thin films, J. Am. Chem. Soc. 124 (2002) 14388–14396.
[11] S.H. Bo, X.H. Liu, Z. Zhen, Preparation and luminescence properties of hybrid materials containing lanthanide complexes covalently bonded to a terpyridine-functionalized silica matrix, J. Lumin. 128 (2008) 1725–1730.
[12] N.N. Lin, H.R. Li, Y.G. Wang, Y. Feng, D.S. Qin, Q.Y. Gan, S.D. Chen, Luminescent triazine-containing bridged polysilsesquioxanes activated by lanthanide ions, Eur. J. Inorg. Chem. 478 (2008) 1–4785.
[13] X.M. Guo, H.D. Guo, L.S. Fu, L.D. Carlos, R.A. Sá Ferreira, L.N. Sun, R.P. Deng, H.J. Zhang, Novel Near-infrared luminescent hybrid materials covalently linking with lanthanide [Nd(III), Er(III), Yb(III), and Sm(III)] complexes via a primary beta-diketone ligand: synthesis and photophysical studies, J. Phys. Chem. C 113 (2009) 12538–12545.
[14] K. Binnemans, Lanthanide-based luminescent hybrid materials, Chem. Rev. 109 (2009) 4283–4374.
[15] C. Molina, R.A. Sá Ferreira, G. Poirier, L.S. Fu, S.J.L. Ribeiro, Y. Messaddeq, L.D. Carlos, Er^{3+}-based diureasil organic–inorganic hybrids, J. Phys. Chem. C 112 (2008) 19346–19352.

[16] B. Yan, H.F. Lu, Lanthanide centered covalently bonded hybrids through sulfide linkage: molecular assembly, physical characterization and photoluminescence, Inorg. Chem. 47 (2008) 5601–5611.
[17] J.L. Liu, B. Yan, Lanthanide, (Eu^{3+}, Tb^{3+}) centered hybrid materials using modified functional bridge chemical bonded with silica: molecular design, physical characterization and photophysical properties, J. Phys. Chem. B 112 (2008) 10898–10907.
[18] H.F. Lu, B. Yan, J.L. Liu, Functionalization of calix[4]arene as molecular bridge to assemble novel luminescent lanthanide supramolecular hybrid systems, Inorg. Chem. 48 (2009) 3966–3975.
[19] L. Guo, B. Yan, Photoactive ternary lanthanide-centered hybrids with schiff-base functionalized polysilsesquioxane bridges and N-heterocyclic ligands, Eur. J. Inorg. Chem. 126 (2010) 7–1274.
[20] P. Liu, H.R. Li, Y.G. Wang, B.Y. Liu, W.J. Zhang, Y.J. Wang, W.D. Yan, H.J. Zhang, U. Schubert, Europium complexes immobilization on titania via chemical modification of titanium alkoxide, J. Mater. Chem. 18 (2008) 735–737.
[21] H.R. Li, P. Liu, Y.G. Wang, L. Zhang, J.B. Yu, H.J. Zhang, B.Y. Liu, U. Schubert, Preparation and luminescence properties of hybrid titania immobilized with lanthanide complexes, J. Phys. Chem. C 113 (2009) 3945–3949.
[22] M.H. Bartl, S.W. Boettcher, E.L. Hu, G.D. Stucky, Dye-activated hybrid organic/inorganic mesostructured titania waveguides, J. Am. Chem. Soc. 126 (2004) 10826–10827.
[23] M. Puchberger, W. Rupp, U. Bauer, U. Schubert, Reaction of metal alkoxides with 3-alkyl-substituted acetylacetone derivatives – coordination vs. hydrodeacylation, New J. Chem. 28 (2004) 1289–1294.
[24] U. Schubert, Chemical modification of titanium alkoxides for sol–gel processing, J. Mater. Chem. 15 (2005) 3701–3715.
[25] S. Ivanovici, H. Peterlik, C. Feldgitscher, M. Puchberger, G. Kickelbick, Atom transfer radical polymerizations of complexes based on Ti and Zr alkoxides modified with beta-keto ester ligands and transformation of the resulting polymers in nanocomposites, Macromolecules 41 (2008) 1131–1139.
[26] R. Hernandez, A.C. Franville, P. Minoofar, B. Dunn, J.I. Zink, Controlled placement of luminescent molecules and polymers in mesostructured sol–gel thin films, J. Am. Chem. Soc. 123 (2001) 1248–1249.
[27] S. Gago, J.A. Fernandes, J.P. Rainho, R.A. Sá Ferreira, M. Pillinger, A.A. Valente, T.M. Santos, L.D. Carlso, P.J. Ribeiro-Claro, I.S. Goncüalves, Highly luminescent tris(beta-diketonate)europium(III) complexes immobilized in a functionalized mesoporous silica, Chem. Mater. 17 (2005) 5077–5084.
[28] L. Armelao, G. Bottaro, S. Quici, M. Cavazzini, M.C. Raffo, F. Barigelletti, G. Accorsi, Photophysical properties and tunable colour changes of silica single layers doped with lanthanide(III) complexes, Chem. Commun. 291 (2007) 1–2913.
[29] J.L. Liu, B. Yan, Molecular construction and photophysical properties of luminescent covalently bonded lanthanide hybrid materials obtained by grafting organic ligands containing 1,2,4-triazole on silica by mercapto modification, J. Phys. Chem. C 112 (2008) 14168–14178.
[30] D.D. Perrin, W.L.F. Armarego, D.R. Perrin, Purification of Laboratory Chemicals, Pergamon Press, Oxford, U.K., 1980.
[31] S.W. Boettcher, M.H. Bartl, J.G. Hu, G.D. Stucky, Structural analysis of hybrid titania-based mesostructured composites, J. Am. Chem. Soc. 127 (2005) 9721–9730.
[32] U. Schubert, E. Arpac, W. Glaubitt, A. Helmerich, C. Chau, Primary hydrolysis products of methacrylate-modified titanium and zirconium alkoxides, Chem. Mater. 4 (1992) 291–295.
[33] B. Yan, Y.L. Sui, J.L. Liu, Photoluminescent hybrid thin films fabricated with lanthanide ions covalently bonded silica, J. Alloys Compd. 476 (2009) 826–829.
[34] M. Saif, M.S.A. Abdel-Mottaleb, Titanium dioxide nanomaterial doped with trivalent lanthanide ions of Tb, Eu and Sm: preparation, characterization and potential applications, Inorg. Chim. Acta 360 (2008) 2863–2874.
[35] E.H. de Faria, K.J. Ciuffi, E.J. Nassar, M.A. Vicente, R. Trujillano, P.S. Calefi, Novel reactive amino-compound: tris(hydroxymethyl)aminomethane covalently grafted on kaolinite, Appl. Clay Sci. 48 (2010) 516–521.
[36] B. Yan, X.F. Qiao, Rare-earth/inorganic/organic polymeric hybrid materials: molecular assembly, regular microstructure and photoluminescence, J. Phys. Chem. B 111 (2007) 12362–12374.
[37] K. Sheng, B. Yan, H.F. Lu, L. Guo, Ternary rare earth inorganic/organic hybrids with mercapto functionalized Si–O linkage and polymer chain: coordination bonding assembly and luminescence, Eur. J. Inorg. Chem. (2010) 3498–3505.
[38] J.M. Lehn, Perspectives in supramolecular chemistry – from molecular recognition towards molecular information processing and self-organization, Angew. Chem. Int. Ed. Engl. 29 (1990) 1304–1319.
[39] M. Kawa, J.M.J. Frechet, Self-assembled lanthanide-cored dendrimer complexes: enhancement of the luminescence properties of lanthanide ions through site-isolation and antenna effects, Chem. Mater. 10 (1998) 286–296.
[40] V. Bekiari, P. Lianos, Strongly luminescent poly(ethylene glycol)-2,2′-bipyridine lanthanide ion complexes, Adv. Mater. 10 (1998) 1455–1458.
[41] B. Yan, Q.M. Wang, First two luminescent molecular hybrids composed of bridged Eu(III)-β-diketone chelates covalently trapped in silica and titanate gels, Cryst. Growth Des. 6 (2008) 1484–1489.
[42] H.R. Li, J.B. Yu, F.Y. Liu, H.J. Zhang, L.S. Fu, Q.G. Meng, C.Y. Peng, J. Lin, Preparation and luminescence properties of in situ formed lanthanide complexes covalently grafted to a silica network, New J. Chem. 28 (2004) 1137–1141.
[43] Z. Wang, J. Wang, H.J. Zhang, Luminescent sol–gel thin films based on europium-substituted heteropolytungstates, Mater. Chem. Phys. 87 (2004) 44–48.
[44] C.M. Granadeiro, R.A.S. Ferreira, P.C.R. Soares-Santos, L.D. Carlos, H.I.S. Nogueira, Lanthanopolyoxometalates as building blocks for multiwavelength photoluminescent organic–inorganic hybrid materials, Eur. J. Inorg. Chem. 508 (2009) 8–5095.
[45] S.S. Nobre, X. Cattoën, R.A. Sá Ferreira, C. Carcel, V.D. Bermudez, M. Wong Chi Man, L.D. Carlos, Eu^{3+}-assisted short-range ordering of photoluminescent bridged silsesquioxanes, Chem. Mater. 22 (2010) 3599–3609.
[46] F.Y. Liu, L.D. Carlos, R.A. Sá Ferreira, J. Rocha, M.C. Ferro, A. Tourrette, F. Quignard, M. Robitzer, Synthesis, texture, and photoluminescence of lanthanide-containing chitosan–silica hybrids, J. Phys. Chem. B 114 (2010) 77–83.
[47] M. Fernandes, V.D. Bermudez, R.A.S. Ferreira, L.D. Carlos, A. Charas, J. Morgado, M.M. Silva, M.J. Smith, Highly photostable luminescent poly(epsilon-caprolactone)siloxane biohybrids doped with europium complexes, Chem. Mater. 19 (2007) 3892–3901.
[48] J.C. Boyer, F. Vetrone, J.A. Capobianco, A. Speghini, M. Bettinelli, Variation of fluorescence lifetimes and Judd–Ofelt parameters between Eu^{3+} doped bulk and nanocrystalline cubic Lu_2O_3, J. Phys. Chem. B 108 (2004) 20137–20143.
[49] O.L. Malta, M.A.L. Couto dos Santos, C. Thompson, N.K. Ito, Intensity parameters of 4f–4f transitions in the Eu(dipivaloylmethane)(3) 1,10-phenanthroline complex, J. Lumin. 69 (1996) 77–84.
[50] R.M. Supkowski, W.D. Horrocks, On the determination of the number of water molecules, q, coordinated to europium (III) ions in solution from luminescence decay lifetimes, Inorg. Chim. Acta 340 (2002) 44–48.
[51] S. Moynihan, R. Van Deun, K. Binnemans, G. Redmond, Optical properties of planar polymer waveguides doped with organo-lanthanide complexes, Opt. Mater. 29 (2007) 1821–1830.
[52] S.S. Nobre, C.D.S. Brites, R.A. Sá Ferreira, V.D. Bermudez, C. Carcel, J.J.E. Moreau, J. Rocha, M. Wong Chi Man, L.D. Carlos, Photoluminescence of Eu(III)-doped lamellar bridged silsesquioxanes self-templated through a hydrogen bonding array, J. Mater. Chem. 18 (2008) 4172–4182.